EXPERIMENTS ON GRADIENT LIMITS FOR NORMAL CONDUCTING ACCELERATORS

Valery A. Dolgashev, SLAC, Stanford, CA 94309, USA

1 INTRODUCTION

The accelerating gradient is one of the crucial parameters affecting the design, construction and cost of next-generation linear accelerators. For a specified final energy, the gradient sets the accelerator length, and for a given accelerating structure and pulse repetition rate, it determines power consumption.

In this paper experimental results and problems related to breakdown damage, pulsed heating, application of new materials, as well as difference between standing wave (SW) and traveling wave (TW) structures will be discussed.

1.1 Early tests

Due to limited available rf power, early high gradient experiments were limited to standing wave structures and short, low group velocity traveling wave structures. In these experiments the structures have reached very high gradients. The highest gradient obtained during the SLAC construction period (1962-1966) is mentioned in [1] for a short accelerating structure in a resonant ring. It is believed that this structure reached an accelerating gradient of 46 MV/m without obvious signs of breakdown. The surface gradient for this structure was about two times larger than the accelerating gradient. Early high gradient research for a linear collider project was published in Novosibirsk in 1978 [2]. A single S-band cavity was tested up to 150 MV/m (2 μs) surface gradient. The gradient was limited not by breakdowns but by field-emission currents. Standing wave structures were tested at different frequencies with reported surface gradient of 340 MV/m (2.5μs, S-band), and 572 MV/m (0.77μs, X-band)[1]. For the TW structures the surface gradient was somewhat lower: 285 MV/m (0.15 μs, X-band) [3]. This gradient was achieved in the first cell of a constant impedance structure after $\sim 10^7$ pulses. Similar results were obtained during "backward" processing of the DS2 structure [4]. There, rf power was fed into an output coupler of this close-to-constant gradient structure and the maximum surface electric field was in the output coupler cell. The mentioned structures were mostly built specifically for these high gradient tests. The testing procedure also was aimed for a maximum achievable gradient. Such parameters as structure damage, breakdown rate (number of pulses without a breakdown) or heavy loading by dark current were not an issue.

1.2 Gradient requirements

There are two linear collider projects that use normal conducting structures: NLC/JLC (SLAC/KEK) and CLIC (CERN). Operating parameters of the NLC/JLC 11.424 GHz accelerating structure are: loaded accelerating gradient, 55 MV/m (unloaded gradient for TW structure 70 MV/m), 270 ns flat top pulse (after structure is filled with rf energy), no degradation of performance during decades of operation, and less than one breakdown per 10^6 pulses per meter [5, 6]. Beam dynamics limits the minimal iris diameter. Damping of deflecting wake field modes complicates the structure design with additional slots and waveguides. Energy upgrade scenarios for the NLC require accelerating structure designs with even higher working gradients. Operating parameters for the CLIC linear collider are: frequency 29.985 GHz, 150 MV/m average loaded accelerating gradient, and 100 ns flat top pulse [7].

1.3 Breakdown damage

With development of more powerful rf sources operational tests of several prototypes of NLC/JLC 1.8 m TW structures started in the late 1990s. Some of them have shown damage with input power $\sim$90 MW and average gradient 50 MV/m (250 ns)[8]. At the CLIC Test Facility, TW 30 GHz copper structures were processed up to accelerating gradients of 70 MV/m (16 ns, surface fields 304 MV/m) with damage in the coupler iris [9]. As a consequence, an extensive experimental and theoretical programs to resolve the problems of high power operation of the accelerating structures were started in SLAC, KEK and CERN. These programs included testing TW and SW accelerating structures, high power waveguides, and single cavities.

1.4 Recent results

Several TW structures with lower initial group velocity and SW structures were built and tested. These structures require half as much power as high-initial-group velocity prototypes for the same gradient. It became obvious that the performance of the these structures was limited by input and output couplers[6]. The importance of significant reduction of magnetic field in couplers was understood and new coupler geometries introduced. All high power systems were reevaluated for an acceptable level of magnetic fields.

Copper was replaced by tungsten in the CLIC TW accelerating structures with great results. These structures were conditioned to very high surface fields ($\sim$330 MV/m, 16 ns) without damage [9].

High gradient tests of a TW structure with 3% initial group velocity and modified couplers started at the end of August 2002 at SLAC. This structure has an input coupler based on a mode launcher and an output coupler with large (3 mm) radius edges at the waveguide-to-coupler-cell iris to reduce the pulsed heating below 30° C (70 MV/m,

400 ns) [10]. This structure was processed in 10^3 breakdowns to $\sim$70 MV/m (400 ns) accelerating gradient without obvious coupler-induced breakdowns. At the time of publication this test is ongoing.

2 RF BREAKDOWN

RF breakdown is a major factor determining the operating gradient of an accelerating structure. It leads to disruption of operation and damage of the surface. Characteristics of rf breakdown and multiple theories of breakdown physics could be found in [1, 11]. The scope of this paper will be limited to properties of rf breakdown that effect accelerating structure design and operation, such as the breakdown rate and the damage induced by the breakdowns. Although these parameters are not independent, the breakdown rate is most probably determined by the amplitudes of surface electric and magnetic fields, geometry, cleanliness and conditioning history, while the damage is more related to power and energy absorbed during a breakdown event.

2.1 General properties of the rf breakdown

RF breakdown is a phenomenon that abruptly and significantly changes transmission and reflection of the rf power directed to the structure under test. Breakdown is accompanied by a burst of x-rays and by a bright flash of visible light. Listed here are some properties of the rf breakdown in TW structures and waveguides [12]:

1. During a breakdown event transmitted power shuts off completely.
2. Time constant of the power shut-off is 20–200 ns.
3. Up to 80% of the incident rf power is absorbed by the arc.
4. Light (emitted from the breakdown site) lasts for several microseconds after the rf pulse. Spectral lines of this light are mostly from neutral copper atoms.

The breakdown behavior of standing wave (SW) structures [1] is very different from that of TW structures. In the TW case, a major part of the rf energy is absorbed by breakdown currents; in the SW case, rf energy is reflected from the structure. After breakdown starts, reflected energy increases during $\sim$100 ns in the TW case, and in $\sim$10 ns in the SW case.

3D and 2D particle-In-Cell simulations of the breakdown dynamics give a possible explanation of the breakdown development [12]. The simulation was based on a model of a "plasma spot"[13]. The breakdown was simulated by creating emission spots in the structure (spot size 2 mm^2...100 mm^2). Space-charge limited emission of electrons from the spot was used. A beam of copper ions was generated in the same area with a predetermined current density. The main results of these simulations for TW structures and waveguides are:

1. The major energy exchange between incident rf fields and particles comes from the interaction of the rf electric fields with electrons (not with ions). Electrons cross the gap in the waveguide or accelerating structure cell in a short time ($\sim$ rf period).
2. The electron current must be several kA to significantly effect the rf power transmission. Space charge-limited emission of electrons without ions cannot produce and sustain the required current densities.
3. Ion currents must be 10–100 A to disrupt the transmitted power. The space charge fields of the ions compensates the electron space charge fields. This compensation allows the generation of kA of electron current. The time constant for the drop off of transmitted power is 10–20 ns and is related mostly to the process of filling the waveguide gap or accelerating structure cell with copper ions.
4. Without electrons, the ions do not move significantly during the rf pulse. In the presence of the space-charge limited electron flow, the ion beam crosses the waveguide in about 30 ns and fills the accelerating structure cell in 20 ns at 60...80 MW of input power. The oscillating space charge field of the electrons adds a dc component to the rf electric field that accelerates the ions.
5. A significant portion (50–80%) of the emitted electrons and ions returns to the emitting spot and the surrounding area.
6. Up to 50% of the input power can be absorbed by the ion-electron beam in the waveguide and up to 60% in TW accelerating structure. To explain the absorption of an additional 20% the model requires the introduction of some effects associated with the interaction of electrons with neutral copper atoms and possible expansion of the emission spot.

The main results of the SW structure simulations are:

1. Electromagnetic fields in the structure collapse just after emission starts. Currents pass across the whole cavity and absorb a major part of the stored rf energy in a few nanoseconds, compared to a filling time of $\sim$100 ns.
2. The currents detune the whole structure, causing the π-resonance to shift from the working frequency. This shift causes rf energy to reflect from the input iris of the structure.

The main conclusion from the experiments and simulations are: 10–100 J of energy deposited by ion-electron currents in a localized spot has big damage potential; SW structures are less likely to be damaged by the breakdowns.

2.2 Damage

Damage in accelerating structures leads to changes in the phase-advance-per-cell in TW structures and in the frequency shift of the π-resonance and changes in distribution of amplitudes in SW structures. Phase advance per cell and resonant frequencies are measured during the high

power processing using rf signals excited by a beam passing through the structures, as well as after the processing using bead-pull techniques. Measurements of the 1.8 m TW prototypes have shown that the input part of the structures is damaged [8]. The output part of these structures had lower local rf power and lower group velocity (5%–2%) and was damaged significantly less than the input part. Further experiments were done with low input group velocity TW structures (5%–3%) and SW structures. The main results of these experiments are:

1. Most of the damage for both TW and SW structures is concentrated in input couplers.
2. There is clear correlation between local *rf power* (or group velocity) and induced damage. For TW structures with 3% group velocity and input power ∼50 MW (400 ns) damage in the body of the structure is barely measurable (but the input coupler is damaged).
3. The *fraction* of the rf pulse energy absorbed in the breakdown arcs (body of TW structures) has no obvious correlation with the total pulse energy, incident power, group velocity or position in the structure.
4. There is no obvious correlation between the absorbed energy and the damage.
5. There is no obvious correlation between the absorbed rf power and the breakdown fields for the low group velocity TW structures. The test structures were designed with constant maximum surface electric fields and a large variation of the group velocity along the structure (5%→3.3%, 3.3%→1.6%, 5%→1.6%, *etc.*). The bodies of the structures(couplers excluded) were broke down uniformly over the length.

The absence of correlation between absorbed rf power and breakdown fields in TW structures is counterintuitive. However maximum gradient in these structures was limited by breakdowns in the couplers. Thus the coupler breakdowns could mask dependence between absorbed power (and energy) and the breakdown fields.

Experiments done at CERN with constant impedance 30 GHz structure (16 ns) have shown severe damage in the coupler on the first structure iris [9]. Location of the damage is well correlated with the maximum surface electric fields.

3 RF BREAKDOWN AND HIGH MAGNETIC FIELDS

3.1 Experiments

There is overwhelming experimental evidence that high magnetic fields induce breakdowns in the couplers of low group velocity TW and SW structures [6]. The maximum gradient in all of these structures was limited by breakdowns in couplers and the damage was concentrated in couplers. Detailed study of the coupler breakdowns has followed.

The breakdowns produce mechanical shock. The shock waves were registered by acoustic sensors [14] installed on the input coupler of a TW structure. The data have shown that the location of the source of the acoustic signal is correlated with the location of waveguide-to-coupler-cell irises.

A video-camera was used to obtain images of the arc in the SW structures. Averaging of more than 100 images shows that the visible arc location, again, corresponds to the location of the waveguide-to-coupler-cell irises. An autopsy of a TW structure has shown that the inner edges (cell side) of the waveguide-to-coupler-cell irises are eroded (see Fig. 1)while the outer edges (waveguide side) are almost intact[15]. Detailed calculations using commercial

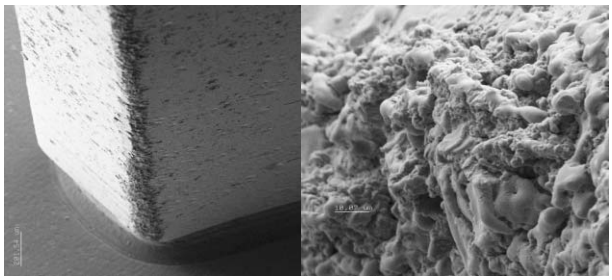

Figure 1: SEM image of inner edges (cell side) of the waveguide-to-coupler-cell irises.

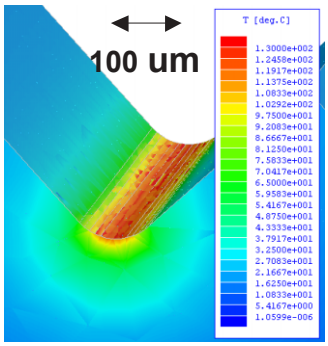

Figure 2: Temperature distribution on the inner edge of the waveguide-to-coupler-cell iris (maximum current 0.7 MA/m, 400 ns).

3D electrodynamics code HFSS^{TM} [16] and a 2D electrostatic code TOPAZ [17] have shown that the surface magnetic field peaked at the inner edge of the iris and reached ∼0.7 MA/m (accelerating gradient 70 MV/m). A simple 1D linear model of rf heating predicts a pulsed temperature rise of $\sim$ 130° C (400 ns) as shown on Fig.2. The accuracy of the temperature calculation is determined by the mechanical tolerances of the small radius ($\sim 80 \pm 30\mu$m) and by the validity of the 2D approximation of the magnetic field distribution. The accuracy is estimated to be $\pm 30\%$. It is unlikely that a temperature rise of $\sim$ 130° C can, by itself, produce breakdowns. Some other phenomena should be present to explain the erosion, acoustic and video data.

Further analysis of the experimental data have shown the following properties of the coupler breakdowns:

1. The breakdown rate is determined by input rf power and pulse width is roughly *constant* over hours and slowly increases.
2. The breakdown rate (number of pulses without breakdown) is roughly independent on the pulse repetition rate.
3. The breakdown rate has a clear correlation with the pulsed temperature, calculated using a primitive model of rf pulsed heating. The breakdown rate has a threshold and grows above the threshold almost exponentially with the temperature. The calculated threshold value is 60–100° C for different accelerating structures.

3.2 Discussion

Mechanical damage due to pulsed heating is discussed in [18, 19]. The model described in [20] suggests that the mechanical fatigue accumulates with each pulse and (after certain number of pulses) macroscopic change occurs (similar to creation of a dislocation). This model is supported by the experimental data on coupler breakdowns with an additional assumption that this macroscopic change triggers the rf breakdown. The physics of the surface heating also needs verification, since other effects, like multipactor discharge in strong magnetic fields, could increase surface the temperature together with ohmic losses. There is experimental data that is not consistent with the simple model of the rf pulsed heating: 5.5 cell X-band rf gun [21] operates with a low breakdown rate (probably, below the pulsed heating breakdown threshold) for the calculated maximum pulsed temperature rise about 130° C.

3.3 Solution

A practical solution of the coupler breakdown problem was obvious: the design of all couplers was changed to reduce pulsed temperature rise below 50° C. Several solutions were introduced [10]: a coupler with increased radius of waveguide-to-coupler-cell iris (to 3 mm from $\sim 80\mu$m); a mode launcher coupler (this coupler has temperature rise $\sim 3^\circ$ C); and a coupler with an rf choke in the rectangular waveguide.

The first two couplers were used in a TW structure with a 3% initial group velocity that is currently under test at SLAC. No noticeable enhancement in the coupler breakdown rates relative to the other cells has been observed at the time of this publication (September, 2002).

Since the effect of high magnetic field was understood, all new high power components were redesigned to reduce the pulsed temperature rise below 50° C.

4 MATERIALS

Use of different metals and alloys for high gradient structures has great potential. Unfortunately, experimental data for materials other than copper are sparse and, sometimes, contradictory. Recent CLIC experiments with a tungsten structure were very successful: the breakdown field was increased up to 340 MV/m (30 GHz, 16 ns) without damage[22]. This experiment clearly shows the advantage of tungsten over copper for short 16 ns pulses and further work is under way to test the structure with the CLIC pulse width of 150 ns.

Tests of waveguides have shown that gold has a lower breakdown field than copper and behaves very similarly to copper waveguide with reduced height [25]. Tests of a 304 stainless steel waveguide have shown a significant increase in the breakdown field and, again, breakdown behavior was different from a copper waveguide of the same geometry: unlike for the copper waveguide, processing of the stainless steel waveguide has been possible with a long (> 400 ns) pulse.

Stainless steel and Glidcop^{TM} were tested in the *windowtron* experiment[11]. Stainless steel performed worse than copper, and this poor behavior was attributed to surface preparation. In spite of good mechanical properties, Glidcop^{TM} had lower breakdown fields than copper. The probable cause for this is aluminum inclusions responsible for good mechanical properties.

Tests of an S-band cavity with noses made of titanium did not show significant improvement in breakdown fields over copper, although dark currents were dramatically decreased[23]. Tests of niobium and SiC in an L-band coaxial cavity have not shown a significant difference from copper[24].

Of all the experiments described above, only the waveguide tests had a pulse energy similar that required for the TW accelerating structure operation. Since stainless steel performed well in this experiment and matches the expansion of copper, it could be incorporated into accelerating structure design. Other materials, such as tungsten (CLIC study is very encouraging) and molybdenum, could also be considered for their high melting temperature and damage resistance and, obviously, need more study.

5 TW STRUCTURES *VS.* SW STRUCTURES

Investigation of the SW option for a linear collider was motivated by early very successful tests of high gradient SW structures and single cavities[1, 11]. Also, experimental study suggested that with lower absorbed power and energy in breakdown arcs, a higher gradient could be reached (low-Q cavity *vs.* high-Q cavities [11], high group velocity *vs.* low group velocity waveguide [25]).

It was expected that SW structures could be conditioned to a higher gradient than the TW structures because the input power for a SW structure is lower than for a TW structure, and narrow-band properties of the SW structure reduce the power-absorbed-in-the-arc. Another advantage of the SW structure is that, unlike in TW structure, the loaded gradient is equal to the unloaded gradient. For NLC param-

eters, this means that the SW structures have to operate at 55 MV/m *vs.* 70 MV/m for the TW structures.

Advantages of TW structures are: 1) fewer couplers per meter of accelerator (a 60 cm TW structure has 2 couplers *vs.* 3 couplers for 60 cm of SW structure); and 2) a conservative and experimentally tested wakefield damping method.

High power tests of 9 low group velocity TW structures (initial group velocity 5%→3%, length 105 cm→20 cm), and 3 pairs of SW structures (15 cells, 20 cm) have shown that the gradient is limited by breakdowns in the couplers and the breakdown damage is concentrated in the couplers [10]. Breakdown rates in the regular cells of these structures were close to the rate acceptable for the NLC.

Since the high gradient in these structures is limited by the couplers, new tests are planned for both SW and TW structures with redesigned couplers (maximum pulsed temperature rise in the couplers $< 50^\circ$ C).

6 DISCUSSION

Low-group-velocity-TW and SW structures with new, low-magnetic-field couplers will, likely, satisfy or exceed NLC requirements, and current experiments with a new TW structure support that. With the coupler problem solved the other phenomena will limit the gradient.

One obvious limitation is the breakdowns due to pulsed temperature rise (δT) in cells other than the coupler cells. The cells become important because the pulsed temperature rise in the new couplers (like mode-launcher-coupler) is lower than in the structure body. The δT in a structure cell is proportional to $E_a^2\sqrt{t_p}/R_{sh}$, where E_a is the accelerating gradient, R_{sh} is the shunt impedance, and t_p is the pulse length. For NLC parameters this gradient is above 160 MV/m (400 ns, $\delta T > 100^\circ$C). Introducing slots for the wakefield damping will reduce this limit. NLC cells with slots are redesigned to keep the value of δT as low as possible [10].

Another limitation for the gradient is the loading of rf power by field emission (dark) currents. This problem was noted in the early experiments [2]. The power P absorbed by the current is a very strong function of the surface fields E_s: $P \sim E_s^\alpha$, where α ranges from 9 to 20. Since, in resent tests of the SW and TW structures, dark-current-loading was not observed with surface electric fields up to 200 MV/m the gradient limited by this phenomena is, likely, above 100 MV/m.

Other limitations, such as possible reduction of breakdown fields with increased absorbed power, are yet to be studied.

7 ACKNOWLEDGMENTS

I greatly appreciate help of: C. Adolphsen, W. Baumgartner, G. Bowden, D. Burke, J. Cornuelle, V. Ivanov, K. Jobe, R. Jones, R. Kirby, L. Laurent, F. LePimpec, J. Lewandowski, Z. Li, R. Loewen, D. McCormick, R. Miller, C. Nantista, C. Ng, C. Pearson, M. Ross, R. Ruth, T. Smith, S. Tantawi, A. Vlieks, J. Wang, P. Wilson of SLAC; Y. Higashi, T. Higo, N. Toge of KEK; W. Wuensch and S. Döbert of CERN.

8 REFERENCES

[1] J.W. Wang, "RF Properties of Periodic Accelerating Structures for Linear Colliders," SLAC-Report-339, Ph.D. Dissertation, Stanford University, 1989.

[2] V.E. Balakin *at al*, "Accelerating Structure of a Colliding Linear Electron-Positron Beam (VLEPP), Investigation of the Maximum Attainable Acceleration Rate," Novosibirsk, Nov., 1978, SLAC-TRANS-0187.

[3] J.W. Wang *at al*, "SLAC/CERN High Gradient Tests of an X-Band Accelerating Section," CERN-SL-95-27-RF, PAC95 , Dallas, TX, May 1-5, 1995.

[4] R. Loewen, "ASTA Structure Operation Results." Presented at Structure Breakdown Workshop, SLAC, August 28 - 30 , 2000.

[5] "2001 Report on The Next Linear Collider," SLAC-PUB-R-571, Snowmass, Colorado, 2001.

[6] "NLC note," July, 2002.

[7] G.Guignard ed., "A 3 TeV e+e- Linear Collider Based on CLIC Technology," CERN 2000-008.

[8] C. Adolphsen *at al*, "RF Processing of X-Band Accelerator Structures at the NLCTA," LINAC2000, August, 2000, Monterey, CA.

[9] W. Wuensch, "High-Gradient Breakdown In Normal-Conducting RF Cavities," EPAC 2002, June 2002, Paris, France.

[10] J. W. Wang *at al.*, "Recent Progress in R&D of Advanced Room Temperature Accelerator Structures," TH464, this conference.

[11] L. Laurent, "High Gradient RF Breakdown Studies," Ph.D. Dissertation, UC Davis, 2002.

[12] V.A. Dolgashev, S.G. Tantawi, "Simulations of Currents in X-band accelerator structures using 2D and 3D particle-in-cell code," FPAH057, PAC 2001, June 18-22, Chicago, Illinois. pp. 3807-3809.

[13] P.B. Wilson, "A Plasma Model for RF Breakdown in Accelerator Structures," LINAC 2000, Monterey, CA, August, 2000.

[14] J. Frisch *at al.*, "Studies of Breakdown in High Gradient X-band Accelerator Structures Using Acoustic Emission," TH484, this conference.

[15] F. Le Pimpec *at al.*, "Autopsy on an RF-Processed X-band Traveling Wave Structure," MO486, this conference.

[16] http://www.ansoft.com/products/hf/hfss/

[17] V. Ivanov, "Computer simulation the problems of high-current electronics," Proc. 11-th IEEE Int. Pulsed Power Conf., Baltimore, Maryland, June 29- July 2, 1997.

[18] O.A. Nezhevenko, "On The Limitations of Accelerating Gradient in Linear Colliders Due to the Pulsed Heating," PAC97, Vancouver 1997, p.3013.

[19] D.P. Pritzkau, "RF Pulsed Heating," SLAC-Report-577, Ph.D. Dissertation, Stanford University, 2001.

[20] V.F. Kovalenko *at al.*, "Thermophysical Processes and Electrovacuum Devices," Moscow, SOVETSKOE RADIO (1975), pp. 160-193.

[21] A.E. Vlieks, "Development of an X-band Photoinjector at SLAC," MO453, this conference.

[22] S. Döbert, "Status of Very High Gradient Cavity Tests," TU202, this conference.

[23] H. Matsumoto, "Dark Currents," LINAC96, 26-30 August, Geneva, Switzerland.

[24] D. Sun, "Electrical Breakdown And Field Emission in RF Cavities," Ph.D. Dissertation, Texas A&M University, August, 1992.

[25] V.A. Dolgashev, S.G. Tantawi, "RF Breakdown in X-band Waveguides," TUPLE098, EPAC'02, 3-7 June, 2002, Paris, France, pp. 2139-2141.